COMP9517 – Assignment 2

Individual Component: Optic Disc segmentation from Fundus Images using Classical Methods

Mark Thomas
z5194597
z5194597@ad.unsw.edu.au

***Abstract*—Optic disc segmentation has a variety of applications which may include ophthalmic pathological diagnosis or as pre-processing step for either Machine Learning or Deep Learning applications. This paper outlines a template-based approach, followed by thresholding for optic localization. For optic disc segmentation, morphological operators and edge detectors were first used, followed by thresholding. The procedure was tested on a subset (54 images) of the 81 images in the IDRiD dataset. The localization procedure succeeded in 100% of the images with respect to 150x150 window. The average computational time was 2 hours and 12 minutes with a standard deviation of 3 minutes. The segmentation had an IOU score of 62.16% with an average computational time of 1 hour and 25 mins with a standard deviation of 2 mins. (*Abstract*)**

Keywords— edge, localization, morphological, segmentation, template, thresholding (*key words****)***

I. Introduction

The optic disc or the optic nerve head (OD) is formed from the convergence of Retinal Ganglion Cells, which are photoreceptive cells that detect changes in light level [1]. It is one of the most significant regions sought after in image processing, as it is subject to a variety of ophthalmic pathologies including glaucoma, toxic optic neuropathy, papilledema [2] which requires careful examination of the disc itself. In other cases, the opposite is required, where the removal of the disc is integral in highlighting other region of interest such as blood vessels, hard exudates, cotton wool spots (soft exudates) etc.

While there are a plethora of techniques, that takes advantage of different implementations of a convolution neural net, this paper focuses on the classical techniques that could inherently perform the task adequately.

The procedure outlined consists of two parts; optic disc localization, followed by optic disc segmentation. OD localization exploits the fact that in most images, the OD is the brightest portion of the image. This remain true even across image of varying brightness. Hence, by isolating the unique spread of RGB intensities that define the OD, it is possible to identify the regions in an image that best correlate with the optic disc.

II. Background

A. Image Dataset

The image set provided for use, is a subset of 54 images full resolution Red, Green, Blue (RGB) images (herin referred to as base images) and their corresponding masks (herin referred to as ground-truth images), both of which were obtained from the Training set of the Segmentation Challenge in the IDRiD database [3]. The collective resolution of these images is 4288x2848 px. The ground-truth masks are binary in nature with Black denoting the background and Red denoting the segmented optic disc. The RGB images have an average file size of 356 KB while the corresponding masks have a file size of 1.46 MB.

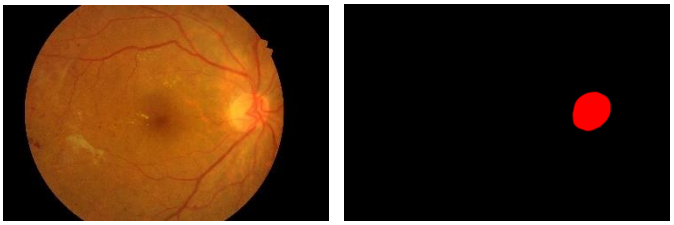

Figure 1: (Left) RGB Image, (Right) Ground-Truth Mask for IDRiD_27 in IDRiD dataset.

Both the base and ground-truth images were converted from the Blue, Green Red (BGR) color space to the RGB color space due to the way that *cv2.imread* reads in images, using the *cv2.cvtColor* function. Then, these images were convolved with a 6x6 average filter to eliminate noise. This was accomplished using the inbuilt function *cv2.blur*.

B. Optic disc Localization

The approach followed was adapted from Dehghani et al., where they indicate that most methods "fail when pathological regions exists in retinal images" [4, p. 3]. The workaround to this is to use a template-based approach where first, an OD window is segmented from a subset of images.

The subset of images selected was 4 out of the provided dataset. This could be construed as the "training step", where the first four images constitute the "training" phase, while the remainder of the dataset is the testing set. The selection of 4 images was subjective, however, through empirical testing these were sufficient for localizing the OD.

An 80 x 80 px OD window was suggested by Dehghani et.al [4, p. 4]. Although, the OD window size is subjective, through empirical testing, it was discovered that on average the OD had a window size of 480x480 for the full resolution base images. Moreover, the resized 80 x 80 OD window was well adapted for the downstream processes and the architecture those processes were tested on. Hence, the original images were, down sampled by a factor of

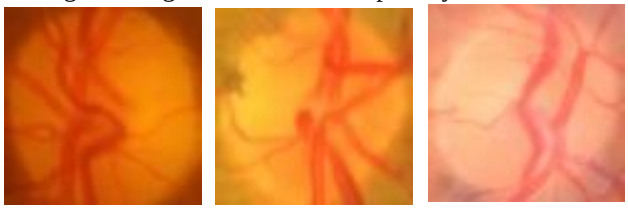

Figure 2: (Left) Dark OD (Middle) Medium OD (Right) Light OD from IDRiD_11, IDRiD_22 and IDRiD_46 in the IDRiD database respectively.

6 to a resolution of 707x470 px. This ensures that OD window extracted is of size 80x80.

These segmented optic discs were then averaged into a singular image with the corresponding Red, Green and Blue component histograms becoming the template. Following this, each image in the dataset is iteratively indexed for a similarly sized 80x80 neighbourhood. For each neighbourhood, a correlation coefficient for each RGB component, denoted as C_{cr}, is calculated (Eq. 1) [4, p. 4]. Moreover, pixel intensities over 200 were discarded for each component, to exclude exudates and similarly matching regions from the template.

$$C_{cr} = \frac{1}{(1 + \Sigma(a_{cr} - b_{cr})^2} \qquad cr \in \{R, G, B\} \qquad \textit{(Eq. 1)}$$

$$C_{(i,j)} = (t_R * C_R) + (t_G * C_G) + (t_B * C_B) \qquad \textit{(Eq. 2)}$$

The correlation coefficient for each color component was then summed for each component to get the overall correlation coefficient for the neighborhood centred on pixel (i, j), with the centre pixel value replaced with this calculated value (Eq. 2) [4, p. 4]. The maximum value of the correlation map generated (Figure X in Appendix), was used to threshold the image as seen in Eq 3. [4, p. 6].

$$Thr = 0.5 * max(C_{MAP}) \qquad \textit{(Eq. 3)}$$

This should result in a singularly segmented object with the centre of momentum of the object signifying the centre of the optic disc, which can then be segmented out of the base image using a 250x250 px window. The size of the window selected was found to empirically aid in further down stream processes for segmenting out the OD.

However, this approach didn't consider several factors including the variability in the shape of optic discs (circular vs elliptical) and the variability in the brightness of the images. This resulted in a thresholded image that included either multiple segmented objects or, in some cases, the exudate was highlighted along with or instead of the OD.

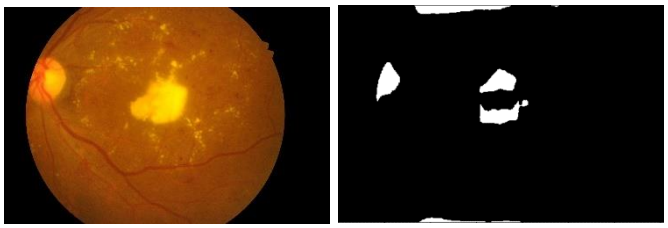

Figure 3: (Left) Base image, (Right) Final thresholded image for IDRiD_10 in the IDRiD database.

To accommodate for these variations, the following additional steps were undertaken. The brightness of the images was considered by counting the number of pixels with a value greater than 127 within a grey-scaled image. Then, the images were sorted based of their count and the first four with the lowest count were considered as the images to be used for the "dark" template (greater than a 18,678-pixel count) and the last 4 were used as the images in the "light" template (less than a 5,051,185-pixel count). To find the template with "medium" brightness, the four closest images to the mean of filtered dataset, 1,074,695-pixel count, were selected (Figure X, Y, Z in the Appendix).

Then, to filter out exudates certain pixel intensity ranges were zeroed out. For the "dark" template, pixel intensities less than 200, greater than 50 and greater than 4 for the Red, Green and Blue component respectively. For the "medium" template, pixel intensities greater than 175, 75 and 50 for the Red, Green and Blue component respectively. For the "light" template, pixel intensities greater than 250, 150 and 77 for the Red, Green and Blue component respectively.

To accommodate for variability in OD size and exudate similarities with respect to their OD, two different connected component functions were computed. One function, *number_of_connected_components_min*, sought to find recursively the minimum threshold factor that would return at least 2 segmented objects. This assumes that if there are two segmented objects, then the largest segmented object would be the optic disc, given the zeroed-out pixel intensity ranges. Conversely, the *number_of_connected_components_max* function, attempted to find if possible a single segmented object. This was possible in "dark" images compared to other images. Finally, the image was thresholded by selecting the half-way mark between the min and max values.

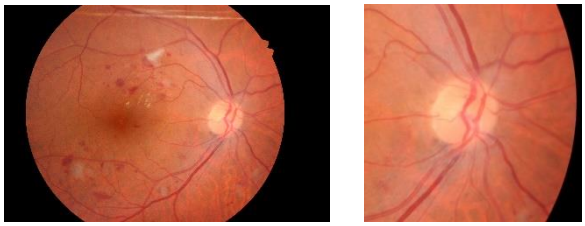

Figure 4: (Left) Base image, (Right) OD window for IDRiD_46 in the IDRiD database.

Finally, the centre of momentum was found for the largest segment object in the image by first, using the Circular Hough Transform in the *sklearn* package to measure the radius of each segment object in the image. Then, the largest radius was selected, and its centre of momentum was obtained.

C. *Optic disc Segmentation*

Once, the optic discs were localized, the approach by Aquino et. Al [5], was used to extract the OD. TO begin with, the authors point out that"blood vessels within the OD act as strong distractors, so they should be erased from the image beforehand." [5, p. 3]. This is accomplished by defining a grey vessel element with a pixel width and a length of 37, which was determined empirically.

The grey vessel element was then rotated 12 times in 15^o increments. Then, for each image, each of the 13 grey-vessel elements were convolved with both the Red and Green component and for each neighbourhood, defined by each grey-vessel element, centred around pixel (i, j), the maximum grey-valued pixel was extracted. Then for the centre pixel (i, j), the maximum value of the set of 13 grey vessel elements was selected.

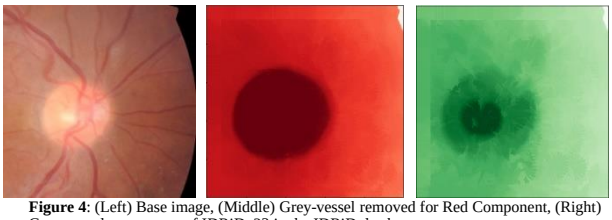

Figure 4: (Left) Base image, (Middle) Grey-vessel removed for Red Component, (Right) Grey-vessel component of IDRiD_23 in the IDRiD database.

Then, the red and green windows, were histogram equalized. They green windows were sharpened with because of the spread if the optic disc in some of the images. The edges were then detected using the Canny Edge detector in the *sklearn* package. The Red and Green images were then eroded and closed using a circular kernel of size 3x3. Finally, the largest circular component was found using Circular Hough Transform, followed by flood fill to extract the component.

III. Experimental Setup

A. Image Dataset

The provided images were form the IDRiD dataset.

B. Experimental Setup

Operating System: Windows 10 Home (Build #: 17134.1040)
Graphics Card: NVIDIA GeForce 940MX
CPU Architecture: Intel® Core™ i7-7500U CPU @ 2.70GHz, 2 Cores, 4 Logical Processors
Installed Ram: 12.0 GB
Python: 3.7.4, OpenCV: 4.1.2-pre (built from binaries), numpy: 1.16.4

C. Metrics (Intersection Over Union)

$$\frac{Area\ of\ the\ Intesection\ Bounding\ Boxes}{Area\ of\ the\ Union\ of\ Bounding\ Boxes}$$

IV. Appendix

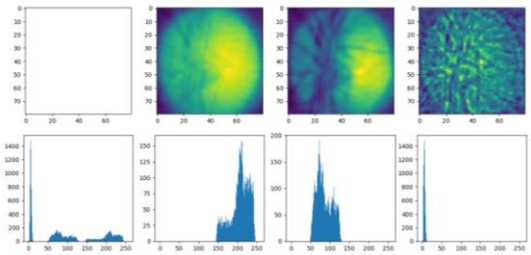

Figure X: (Top) Grey-scaled images, (from left to right) Mean "dark" template of the IDRiD_2, IDRiD_11, IDRiD_25 and IDRiD_35 images in the IDRiD dataset, Red Component of the "dark" template, Green Component of the "dark" template and Blue Component of the "dark" template. (Bottom) The respective histograms of the top row.

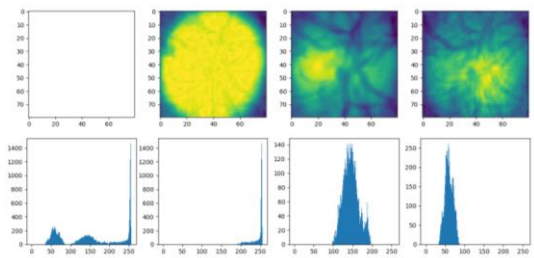

Figure Y: (Top) Grey-scaled images, (from left to right) Mean "medium" template of the IDRiD_18, IDRiD_22, IDRiD_41 and IDRiD_52 images in the IDRiD dataset, Red Component of the "medium" template, Green Component of the "medium" template and Blue Component of the "medium" template. (Bottom) The respective histograms of the top row.

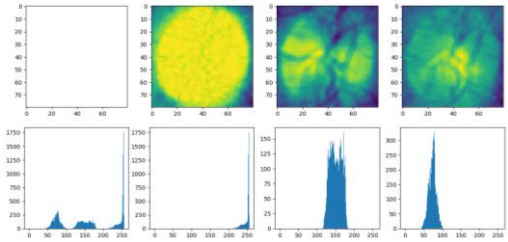

Figure Y: (Top) Grey-scaled images, (from left to right) Mean "light" template of the IDRiD_8, IDRiD_16, IDRiD_46 and IDRiD_53 images in the IDRiD dataset, Red Component of the "light" template, Green Component of the "light" template and Blue Component of the "light" template. (Bottom) The respective histograms of the top row.

References

[1] J. J. Salazar, A. I. Ramírez, R. D. Hoz, E. Salobrar-Garcia, P. Rojas, J. A. Fernández-Albarral, I. López-Cuenca, B. Rojas, A. Triviño, and J. M. Ramírez, "Anatomy of the Human Optic Nerve: Structure and Function," *IntechOpen*, November 2018.

[2] S. Prasad, N. J. Volpe, and L. J. Balcer, "Approach to Optic Neuropathies," The Neurologist, vol. 16, no. 1, pp. 23–34, 2010.

[3] Prasanna Porwal, Samiksha Pachade, Ravi Kamble, Manesh Kokare, Girish Deshmukh, Vivek Sahasrabuddhe, Fabrice Meriaudeau, "Indian Diabetic Retinopathy Image Dataset (IDRiD)", IEEE Dataport, 2018. [Online]. Accessed: 5th November 2019.

[4] A. Dehghani, H. A. Moghaddam, and M.-S. Moin, "Optic disc localization in retinal images using histogram matching," EURASIP Journal on Image and Video Processing, vol. 2012, no. 1, August 2012.

[5] A. Aquino, M. E. Gegúndez-Arias, and D. Marín, "Detecting the Optic Disc Boundary in Digital Fundus Images Using Morphological, Edge Detection, and Feature Extraction Techniques," IEEE Transactions on Medical Imaging, vol. 29, no. 11, pp. 1860–1869, 2010.

[6]